

## PHYSICALLY BASED HYDROLOGICAL MODELLING OF INLAND EXCESS WATER

Boudewijn VAN LEEUWEN<sup>1</sup>, Tamás PRÁVETZ<sup>1</sup>,  
Zoltán Árpád LIPTAY<sup>2</sup> & Zalán TOBAK<sup>1</sup>

<sup>1</sup>University of Szeged, Department of Physical Geography and Geoinformatics, Egyetem utca 2, Szeged, HU 6722, Hungary, leeuwen@geo.u-szeged.hu, pravetz@gmail.com

<sup>2</sup>University of Pécs, Institute of Geography, Ifjúság útja 6, Pécs, HU 7624, Hungary, zoltanarpad@gmail.com

**Abstract:** Large areas of the Carpathian Basin are susceptible to inland excess water due to superfluous precipitation in combination with insufficient infiltration, evaporation and runoff. The modelling of areas threatened by these floods is nowadays often GIS based, using conceptual modelling techniques, where the risk/hazard of inland excess water is determined based on a set of weighted GIS and/or remotely sensed data layers each representing a specific factor. This type of modelling is difficult to verify and apply in other areas. To avoid these problems, in this research, a numerical approach is presented where a hydrological model is applied to determine inland excess water development. The input data have been determined by measurements of physical phenomena. The advantages of our approach are that (1) simulated inland excess water inundations can be verified with actual flood data, (2) physical computations can be repeated in other areas susceptible to inland excess water as well, and (3) the model can be used to calculate different scenarios simulating the impact of human intervention in inland excess water. This study shows the applicability of the approach for inland excess water modelling and aims to determine its data requirements and limitations. The results are compared to inundations digitized from a high resolution satellite image and show that the method gives accurate results using the available data.

**Keywords:** Inland excess water; physically based modelling; flood. runoff, infiltration

### 1. INTRODUCTION

For the coming 50 years, most climate models predict a stable yearly amount of precipitation for the Carpathian Basin, but this precipitation will increasingly fall during extreme precipitation periods (Mezősi et al., 2014). During these periods, in areas with limited runoff, infiltration and evaporation the superfluous water remains on the surface. This type of flood is often identified as inland excess water, surface ponding, areal flood or surface water flood. In Hungary, on average, every year 110 000 ha of land is covered with inland excess water, but since 1935 there have been 10 years with less than 10 000 ha, and 14 years with more than 200 000 ha of land covered with water. In recent years, the most extreme inundations occurred in 1999 (445 000 ha) and 2011 (355 000 ha), resulting in large financial losses (Szatmári & Van Leeuwen 2013). The floodings mostly occur in rural

areas where the inundations cause a decrease in quantity and quality of agricultural goods, and higher costs for agricultural production and for mitigation of inland excess water in the short term, and soil degradation (deterioration of the soil texture, salinization, compaction) on the long term.

The main factors influencing the development of inland excess water are meteorological, relief and geomorphology, soil, groundwater, land use and land cover, and other anthropological factors. The meteorological factor is the determining dynamic factor in the development of inland excess water. It consists of precipitation, temperature, humidity and wind speed. Precipitation is the source for inland excess water. Its amount, intensity and interval control the severity of the inundations. Temperature, humidity and wind speed regulate the evaporation of surplus water.

Relief is the most important static factor for the formation of inland excess water. Surface runoff

towards rivers is hardly occurring in areas with small relief differences; instead the water is accumulating in local depressions, like in former meanders that are often only a few decimetres lower than their surroundings.

The infiltration capacity of the soil is determined by its physical and chemical characteristics. The compactness, particle composition, clay mineral composition, organic matter content, storage capacity are all important factors in the development of inland excess water (Gál & Farsang 2013). The condition of the soil is also important for the formation of the inundations. Even on soil without physical or chemical degradation inland excess water can occur if the soil is saturated due to earlier rainfall periods or frost. Soil can also be degraded as a result of improper agricultural practices like repetitive ploughing at the same depth causing a plough pan or due to over-irrigation. High groundwater levels can result in the formation of inland excess water; when soils allow for the horizontal movement of water, upwelling inland excess water can develop at locations where groundwater appears on the surface in local depressions or at places where there is a sudden decrease in height (e.g. at the border of an alluvial fan, at a channel incision). Furthermore, in areas where groundwater is close to the surface, small variations in the groundwater level may lead to inland excess water (Van Leeuwen 2012).

The surface permeability is strongly related to the land cover. Rural areas normally have less sealed surfaces compared to urban areas with paved roads, car parks etcetera. In urban areas, runoff is normally organized with a dense network of artificial channels, while in rural areas the runoff is often happening through a system of (natural) ditches and channels. The construction of roads and other infrastructure can disturb the natural runoff, may compact soils and can disturb groundwater movement resulting in an increased chance of inland excess water (Barta et al., 2011). In many areas that were historically considered as (semi-permanent) wetlands, nowadays agricultural activities are executed. In these areas, in the past, floods were considered a natural phenomenon, while now they are considered a harmful process (Rakonczai et al., 2011). Many of these areas, extreme rainfall, combined with snow melt, cause inland excess water at the end of the winter, while in summer high temperatures and very low precipitation amounts cause drought. Rigorous drainage of these areas to solve the inland excess water problem might cause aridification in the long term (Romanescu et al., 2011). Careful water management policies are

required to reach a balance between the surplus of water during the wet periods and the shortage of water in the dry periods (Romanescu 2009). Policies towards reappreciation of wetlands, storing inland excess water to use it during dry periods (Szatmári & Van Leeuwen 2013) and using wetlands to diminish river floods (Romanescu 2009) are getting increased attention.

Inland excess water types can be categorized based on the direction of the water flow (Rakonczai et al., 2011). The most common type is accumulative inland excess water, where the surplus of water accumulates under gravity in local depressions due to limited infiltration and evaporation. This happens in areas with very low relief intensity. The height differences are often smaller than a few decimetres. Unfavourable soil characteristics results in low infiltration capacity.

The second type is the upwelling inland excess water, where groundwater flowing towards lower areas, appears on the surface by leakage through porous soil. This normally occurs at the edges of alluvial fans, between ridges in the middle of the fan or at areas where the natural ground water table is close to the surface.

The third type of inland excess water occurs due to queuing up of inland excess water when surplus water is transported away via a system of open drainage channels towards a pumping station which pumps the water into a main river. If the capacity of the pumping station is not sufficient, the water queues up in front of the pumping station causing floods on the land directly surrounding the drainage channels.

Although inland excess water got most scientific attention in Hungary, the phenomenon is not limited to this geographic region. For example, in China, Germany, India, Italy, the Netherlands, Serbia, Romania and Russia, it occurs as well (Kuti et al., 2006, Romanescu et al., 2011). In literature, no unambiguous term exists to describe the phenomenon; terms that have been used in international literature are inland excess water, excess water, surface ponding, areal flood and surface water flood (Priest et al., 2011, Van Leeuwen 2012).

Studying inland excess water is important for three main reasons; (1) to understand the interrelated factors and processes that cause the formation of inland excess water, (2) determination of the location and size of the inundation to be able to take operative measurements to mitigate and prevent further damage, and (3) forecasting the location, size and duration of future floods to develop preventive policies.

Scientific research and operational treatment of inland excess water has focused on its theoretical background (Szatmári & Van Leeuwen 2013, Barta et al., 2011, Rakonczai et al., 2011), monitoring and mapping (Klink & Bálint 2009, Pásztor et al., 2014, Túri & Szabó 2012, Van Leeuwen et al., 2012), modelling (Bozán et al., 2009, Van Leeuwen 2012), prediction, and prevention or mitigation (Priest et al., 2011) of the phenomenon.

Two main approaches of modelling of areas threatened by inland excess water can be identified. The first approach is a geographic information system (GIS) based conceptual modelling technique, where the risk/hazard of inland excess water is determined based on a set of weighted data layers each representing a specific factor, like relief, soil, precipitation etcetera. Examples of this approach are Bozán et al., (2009) and Pásztor et al., (2014). The result of the GIS based approach is a map giving an index indicating the sensitivity of an area to inland excess water based on the given parameters. The weight of the individual parameters is determined based on expert knowledge or multiple regression analysis using an inland excess water frequency map as dependent variable. The weighing factors are only valid in the study area and can therefore not be generalize to other geographic areas in order to predict inland excess water. The second approach is based on remotely sensed data which is processed using classification methods or by calculation indices (e.g. NDVI, Tasseled cap wetness index) into categories like inland excess water, saturated soil, dry soil and vegetation in water (Csornai et al., 2000, Mucsi & Henits 2010, Van Leeuwen et al., 2012, Túri & Szabó 2012, Romanescu et al., 2011). This approach results in maps showing inland excess water at the moment the aerial photograph or satellite image was taken, but cannot provide information on the status of the inundation in the future. The method is limited by the availability of data; passive remote sensing data can only be collected in cloud free circumstances and satellite data in general is limited in temporal resolution due to the orbit of the satellite. Aerial photography is often also weather dependent, needs to be planned in advance and is relatively expensive (Van Leeuwen 2012).

This research applies a hydrological model to determine inland excess water development using a numerical approach. The model is the MIKE SHE model - developed by DHI – which can be used to calculate surface and groundwater movement based on physical parameters. Based on data on the past and current situation, the model can be calibrated to provide new insights in the development of inland

excess water and can predict the extent, location and duration of future floods.

Hydrological models always demand a large amount of input data. The primary focus of the study is to determine the applicability of the approach for inland excess water modelling and to determine its data requirements and the possible limitations.

If the model proves to be usable for inland excess water modelling, it clearly has incomparable advantages over other models based on more static methods. The dynamic and purely physical based simulation of a phenomenon includes the possibility to generate different scenarios, e.g. modelling of human impact on a natural domain which has an unavoidable effect on the movement of water in the catchment, or even forecasting future situations based on predicted input data. All these features are welcomed by engineers during designing processes, moving forward to parallel designing using a dynamic modelling tool to validate the designed elements.

## **2. TOOLS AND METHODS**

### **2.1. Description of the model**

Numerical hydraulic and hydrologic modelling is based on two pillars. The first is the physical system, or its representation, and the other consists of the processes acting on the system and their descriptions. Hydrological models are therefore categorized according to these two aspects (Davie 2008). On one hand, a hydrological model can be seen as a system with cumulative parameters, where the physical system is treated as one integrated unit. On the other hand, it can be seen as a distributed parameter model, where the physical system is divided into calculation units (usually as a grid) and where for each individual computing cell a specific set of parameters exists. The way the processes are described can also be grouped in multiple ways. They can be described as deterministic or stochastic models, or as physics based conceptual and empirical models. Each group has its own data requirements, computational demands and accuracy, and therefore each group has its own applicability.

The aim of this research is the detailed modelling of the physical basis of inland excess water formation and to determine the possibilities for forecasting the phenomenon. For these purposes, an integrated hydrological model with distributed parameters, called MIKE SHE (System Hydrologique European), was used.

The model simulates the water movements via five submodels, but the individual submodels are

embedded into each other, ensuring the incorporation of the dynamic interaction between them, which would not be possible in a simple serial structure (Graham & Butts 2005). For inland excess water modelling this is essential, since also in reality this phenomenon is the results of a complex set of interrelated factors. The following sections describe the five submodels. Figure 1 shows a schematic diagram of the structure of the model.

### 2.1.1. Overland flow

The movement of water resulting in accumulation on the surface can be modelled in MIKE SHE using two different approaches (Danish Hydraulic Institute 2014b). The simplest approach is a one-dimensional calculation using the steepness of the slope and the surface roughness within one subcatchment. The other approach is a finite difference method, which is based on the two-dimensional St. Venant equations diffusion-wave approximation. For this study, the 2D approach was required, because the aim was to calculate the formation of local inundations, and not the determination of the runoff within a catchment. The calculations are applied to a rectangular grid, and one of the aims of this study was to determine the optimal resolution of that grid.

MIKE SHE uses rectangular Cartesian ( $x, y$ ) coordinates on the horizontal plane, with  $z_g(x, y)$  as ground surface level,  $h(x, y)$  as flow depth and  $u(x, y)$  and  $v(x, y)$  as flow velocities in the  $x$ - and  $y$ -directions, and  $i(x, y)$  as the net input into overland flow. The conservation of mass gives:

$$\frac{\partial h}{\partial t} + \frac{\partial}{\partial x}(uh) + \frac{\partial}{\partial y}(vh) = i \quad (1)$$

The momentum equations with the introduction of Strickler/Manning-type law for each friction slope, and simplification of the diffusive wave approximation of two-dimensional St. Venant equations, the relationship between the velocities and the depths may be written as:

$$uh = K_x \left(-\frac{\partial z}{\partial x}\right)^{1/2} h^{5/3} \quad (2)$$

$$vh = K_y \left(-\frac{\partial z}{\partial y}\right)^{1/2} h^{5/3} \quad (3)$$

Where  $uh$  and  $vh$  represent discharge per unit length along the cell boundary in  $x$ - and  $y$ -directions,  $z$  representing the absolute water level ( $z_g + h$ ), and  $K_x$  and  $K_y$  are Strickler coefficients in the two directions with typical values ranging from 10 (densely vegetated channel) to 100 (smooth channel).

To solve the above equations, a wide range of numerical schemes are known. MIKE SHE uses the Finite Difference Formulation with either the Successive Over-Relaxation (SOR) Numerical Solution consisting of a linear matrix system of equations and unknown water levels solved iteratively using a modified Gauss Seidel method, or the Explicit Numerical Solution consisting of the 3-step calculation of flow rates between overland cells and river links, maximum allowed time steps based on given stability criteria (e.g. Courant, Cell volume, etc.) and finally the calculation of actual flows between all the cells and to/from the river links.

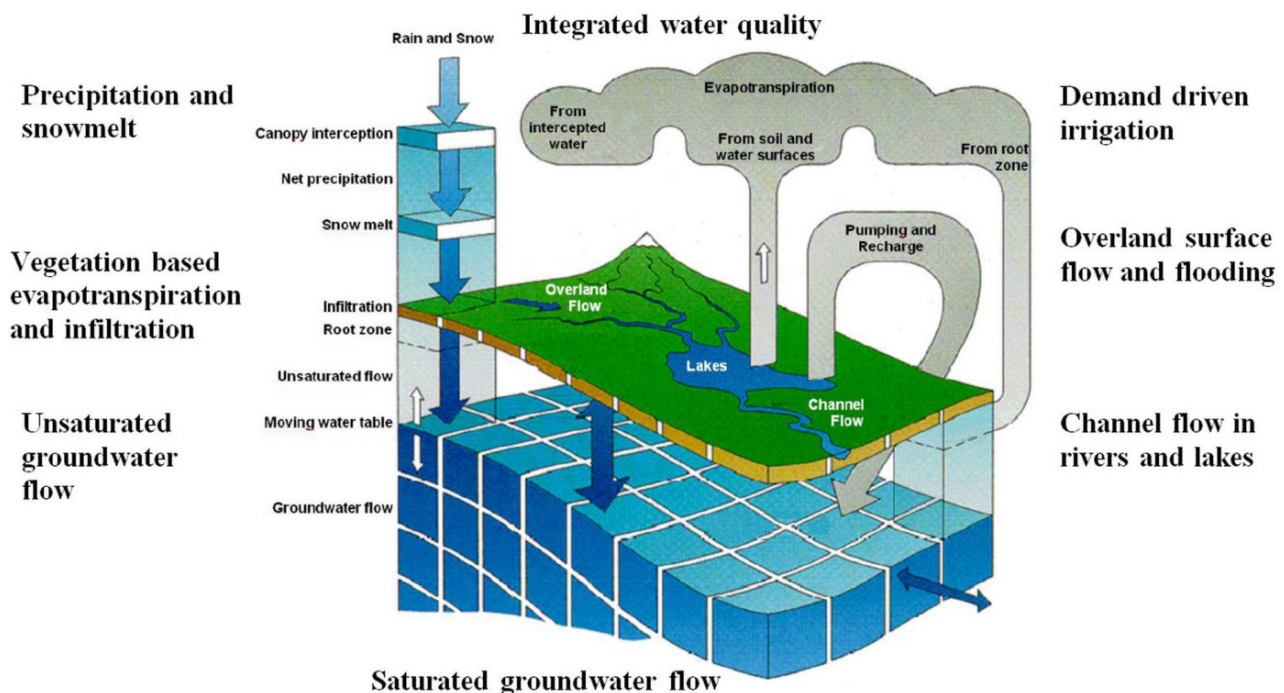


Figure 1. Structure of the MIKE SHE model (Danish Hydraulic Institute 2014a).

The model has a special feature called the low gradient damping function making the model a good choice for inland excess water studies. Due to the Courant criteria at low or nearly zero water depth difference between adjacent cells, the calculation time step also goes to zero, which would lead to less stable and long calculations. The damping here acts like increased resistance between the cells reducing the flow, leading to more stable calculations and longer time steps.

### 2.1.2. Channel flow

It was necessary to model the channel flow with a different method than the overland flow because the resolution of the computational mesh was often smaller than the width of the rivers, streams and riverbed channels. Therefore, the MIKE 11 one-dimensional hydrodynamic model – which is an integrated part of MIKE SHE – was used to model the flow within the network of inland excess water channels. An example of the before mentioned dynamic interaction is the connection between the groundwater and the channel flow, which can only be modelled with similar embedded sub-models. Due to the small height differences in the study area, the inland excess water channels are primarily fed by an increase of the groundwater level and not by surface runoff. The groundwater - channel flow relationship is represented in the model.

The MIKE 11 HD model solves the vertically integrated St. Venant equations, the continuity and momentum equations, or the conservation of mass and energy as widely known:

$$\frac{\partial Q}{\partial x} + \frac{\partial A}{\partial t} = q \quad (4)$$

$$\frac{\partial Q}{\partial t} + \frac{\partial \left( \alpha \frac{Q^2}{A} \right)}{\partial x} + gA \frac{\partial h}{\partial x} + \frac{gQ|Q|}{C^2 AR} = 0 \quad (5)$$

Where  $Q$  represents the discharge,  $A$  the flow area,  $q$  the sum of lateral inflows,  $h$  the stage above datum,  $C$  the Chezy resistance coefficient,  $R$  the hydraulic radius and  $\alpha$  represents the momentum distribution coefficient. The above equations are based on five general assumptions: (1) the water is incompressible and homogeneous, (2) the bottom slope is small, thus the cosine of the angle it makes with the horizontal may be taken as 1, (3) the wavelengths are large compared to the water depth, ensuring that flow everywhere can be regarded as having a direction parallel to the bottom, vertical accelerations are neglected and a hydrostatic pressure variation along the vertical can be assumed, and (4) the flow is subcritical.

The solution scheme of the MIKE 11 model is based on an implicit finite difference scheme. The

computational grid is an alternating type with discharge and water level calculation points. It is automatically generated based on the user defined geometrical data such as cross-profiles and the network of river beds. In order to obtain stable and accurate solutions from the finite difference scheme, the model applies a group of stability criteria, generally included in the Courant condition:

$$C_r = \frac{\Delta t(V + \sqrt{gh})}{\Delta x} \quad (6)$$

Where  $V$  represents the velocity,  $\sqrt{gh}$  is the wave celerity of a small disturbance in shallow water with  $h$  as water level and  $g$  as gravitational constant,  $\Delta t$  is the time step, and  $\Delta x$  is the topographical resolution meaning the distance of calculation points.

The main role of MIKE 11 integration in MIKE SHE in case of inland excess water modelling is to simulate the exchange between the water in the river bed and the connecting ground water table. The models handle this interaction as a simple conductance written as:

$$Q = C * \Delta h \quad (7)$$

Where  $Q$  represents the exchange flow,  $\Delta h$  the head difference between the river and the neighbouring grid cell. The conductance value,  $C$ , is dependent on model settings; it could be a function of the horizontal hydraulic conductivity of the grid cell and the facing grid size, if the river bed is in full contact with the aquifer, or a function of the leakage coefficient of the bed material and wetted cross-section perimeter, if the head loss of the aquifer may be ignored (e.g. if the bed material is thick and very fine and the aquifer material is coarse), or both, if exchange flow can be assumed both from the river bed and from the aquifer. In this last case,  $C$  is written as a serial connection of the individual conductances:

$$C = \frac{1}{\frac{ds}{K * da * dx} + \frac{1}{L_e * w * dx}} \quad (8)$$

Where  $K$  is the horizontal hydraulic conductivity in the grid cell,  $da$  is the vertical surface available for exchange flow,  $dy$  is the grid size used for saturated zone modelling,  $ds$  is the average flow length,  $L_c$  is the leakage coefficient of the bed material, and  $w$  is the wetted perimeter of the cross-profile.

The exchange of water between the river bed and the overland flow is generally handled in a much simpler way compared to ground water exchange. The bidirectional communication of overland water is described by overland spilling, defining the exchange flow by the standard weir formula written

as:

$$Q = \Delta x * C * (H_{us} - H_w)^k * \left[ 1 - \left( \frac{H_{ds} - H_w}{H_{us} - H_w} \right)^k \right]^{-0.385} \quad (9)$$

Where  $Q$  is the flow across the weir,  $\Delta x$  is the cell width,  $C$  is the weir coefficient,  $H_{us}$  and  $H_{ds}$  refer to the height of water on the upstream and downstream side of the weir,  $H_w$  is the height of the weir and  $k$  is a head exponent.

The direct exchange between unsaturated zone and river bed is not implemented in the model. It can be simulated indirectly via overland water accumulation and infiltration or ground water.

### 2.1.3. Unsaturated flow

The model incorporates three methods to calculate the water balance in unsaturated soil (Danish Hydraulic Institute, 2014b). The first is the vertical one-dimensional Richards equation, where the change in the piezometric pressure level is the main driving force behind the movement of water. The pressure level is determined by multiple simultaneous processes, like capillary forces, adsorption between the soil particles and water molecules and gravity. The second method is a simplified form of the Richards equation, where the gravity is the only force. For both methods, it is necessary to provide the soil permeability coefficients based on the water content and the water retention properties at each pressure level. This data can be entered directly, but the model also includes built-in empirical relationships, like the Van Genuchten model, which is a continuous function describing the relationship. The third method is the so-called two layer water balance method, a conceptual model, which main purpose is the determination of the evapotranspiration and groundwater recharge. In this study, the vertical one-dimensional Richards equation was used.

The Richards equation incorporates Darcy's law for volumetric flux, the conservation of mass and the concept of soil water capacity.

$$C \frac{\partial \psi}{\partial t} = \frac{\partial}{\partial z} \left( K(\theta) \frac{\partial \psi}{\partial z} \right) + \frac{\partial K(\theta)}{\partial z} - S \quad (10)$$

Where  $C$  represents soil water capacity,  $\psi$  the pressure head component,  $z$  the gravitational head,  $K(\theta)$  the unsaturated hydraulic conductivity, and  $S$  is the root extraction term.

### 2.1.4. Saturated groundwater flow

The model has two approaches to calculate groundwater movement (Danish Hydraulic Institute, 2014a). The first is a detailed three-dimensional finite difference method, while the second is a

conceptual model based on subcatchments. For inland excess water modelling, the detailed calculations are required, where for every grid cell the groundwater level and flow towards the neighbouring cells is calculated. For this purpose, it is necessary to provide data on the soil stratification, the thickness of the soil horizons and the hydraulic and hydrological characteristics.

The governing flow equation for three-dimensional saturated flow in saturated porous media is:

$$\frac{\partial}{\partial x} \left( K_{xx} \frac{\partial h}{\partial x} \right) + \frac{\partial}{\partial y} \left( K_{yy} \frac{\partial h}{\partial y} \right) + \frac{\partial}{\partial z} \left( K_{zz} \frac{\partial h}{\partial z} \right) - Q = S \frac{\partial h}{\partial t} \quad (11)$$

Where  $K_{xx}$ ,  $K_{yy}$ ,  $K_{zz}$  are the hydraulic conductivity along the x,y,z axes,  $h$  is the hydraulic head,  $Q$  is the source/sink term, and  $S_s$  is the specific storage coefficient. The 3-dimensional Darcy equation is then solved by an iterative implicit finite difference technique.

### 2.1.5. Evapotranspiration

There are two ways to determine the evapotranspiration in the model (Kristensen & Jensen 1975, Danish Hydraulic Institute 2014b). The first is simply to specify the net precipitation ratio, the second uses the Kristensen-Jensen method. For the latter, it is necessary to supply vegetation zone characteristics and particular characteristics of the type of vegetation, such as root depth, leaf area index (LAI) and reference evapotranspiration values.

In the Kristensen and Jensen method, the actual evapotranspiration and the actual soil moisture status in the root zone is calculated from the reference evaporation rate, along with maximum root depth and leaf area index for the plants. The method includes the calculation of evapotranspiration from snow, the canopy interception, the evaporation from the canopy, plant transpiration and soil evaporation.

The evaporation from snow is a sum of the evaporation from the wet and dry snow storages of the model. First the evaporated amount is removed from the wet storage based on the reference evaporation, and if there is insufficient wet snow storage, it will be also removed from the dry snow as sublimation, using the  $S_f$  sublimation reducing factor due to the extra energy required to sublimate snow.

$$ET_{snow} = \underbrace{ET_{ref} * \Delta t}_{\text{wet}} + \underbrace{ET_{ref} * S_f * \Delta t}_{\text{dry}} \quad (12)$$

The canopy interception ( $u_{max}$ ) is simply the

storage calculation using the current LAI of the vegetation and an interception coefficient ( $C_{int}$ ) describing the storage capacity of the vegetation, simulation the retention of precipitation on leaves, branches, and stems of vegetation.

$$I_{max} = C_{int} * LAI \quad (13)$$

If there is water in the canopy storage the canopy evaporation ( $E_t$ ) is also calculated.

$$E_t = \min(I_{max}, ET_{ref} * \Delta t) \quad (14)$$

The transpiration from the vegetation ( $E_{at}$ ) is calculated from the density of the crop green material (LAI) and the soil moisture content in the root zone ( $\theta$ ) and the root density (RDF).

$$E_{at} = f_1(LAI) * f_2(\theta) * RDF * ET_{ref} \quad (15)$$

Where  $f_1$  and  $f_2$  are functions expressing the dependency of transpiration on the leaf area and moisture content based on empirical parameters. The Root Distribution Function (RDF) is a simulation of the complex time-varying distribution of roots determined by the root depth and vertical root density. It handles whether the water is taken from the saturated zone, if the root zone is connected to the water table or distributed between the unsaturated and saturated zones, if capillarity is allowed by the unsaturated zone model (Richards equation or simplified gravity flow).

The soil evaporation ( $E_s$ ) occurs from the upper part of the unsaturated zone and consists of a basic amount of evaporation plus additional evaporation from excess soil water as the soil saturation reaches the field capacity.

$$E_s = ET_{ref} * f_3(\theta) + (ET_{ref} - E_{at} - ET_{ref} * f_3(\theta)) * f_4(\theta) * (1 - f_1(LAI)) \quad (16)$$

Where  $f_3$  and  $f_4$  are functions expressing the dependency of soil evaporation on excess soil water based on empirical parameters and soil saturation thresholds such as the field capacity of the soil. For the above mentioned empirical parameters the model gives estimated values for the different circumstances.

### 2.1.6. Adaptation of the model to the study area

MIKE SHE is generally known as an integrated catchment model with a flexible space and time scaling making it usable for a wide range of applications from greater to local scales both spatially and temporarily.

Since the processes responsible for the development of inland excess water each have a different time scale, this also needs to be represented in the modelling. Every submodel in MIKE SHE

works with its own temporal resolution, and in addition, an automatic time step control algorithm adjusts the size of the time steps according to stability conditions and user specific parameters (Danish Hydraulic Institute 2014a).

This automatism allows fine resolution modelling to be still stable and to have reasonable calculation times necessary in practical usage. Thus no special adaptation of the modelling method was needed for the modelling of the inland excess water phenomenon at such a local scale as presented in this study, only the selection of proper submodels and simulation methods of the physical processes governing it was necessary, since the scales applied later are far away from breaking any assumptions or limiting conditions made during the definition of the basic formulations or empirical factors.

## 2.2. Data

### 2.2.1. Study area

The study area is a 39 km<sup>2</sup> region between Orosháza, Kardoskút and Székkutas (Fig. 2). During the period between March till April 2013, the area was suffering from inland excess water inundations covering a total area of approximately 3.8 km<sup>2</sup>.

The area is flat; height differences of only a few decimetres are typical. A dense network of inland excess water drainage channels is available. The largest channel is the Sóstó main channel, which runs through the east part of the area. Main land use types are natural grass land and non-irrigated agriculture.



Figure 2. Satellite image of the study area (8 April 2013) and its location in Hungary.

### 2.2.2. Digital elevation model

MIKE SHE needs a high resolution digital elevation model (DEM) as input. A DEM with a spatial resolution of 1 meter was created for the study area based on LIDAR data.

On 19 November 2009, an airborne laser scanning flight campaign was executed to collect

LIDAR data from the south-east of Hungary. From a flying height of 1 500 meters, 70 km<sup>2</sup> of terrain was surveyed with an average point density of 1.4 points/m<sup>2</sup>. In total 106 million points were collected. The accuracy of the LIDAR points was evaluated on two test areas for a total number of 15 000 points. The RMSE error for all points was 4.6 cm, while 99.76 % of them were within the specified vertical system accuracy of 15 cm. The maximum vertical error was 22 cm (Szatmári et al., 2012). At the same time of the height recordings, stereo near infrared and colour aerial digital photographs were collected. The resolution of the photographs is 15 cm. Based on the stereo images linear features were digitized in three dimensions using stereo photogrammetric techniques. These break lines were integrated with the original LIDAR measurements, providing more accurate height information of anthropogenic structures in the terrain (Szatmári et al., 2012). The raw LIDAR points and the 3D objects were converted to a raster DEM (Fig. 3).

### 2.2.3. Along and cross sections of the drainage channels

In the study area, many inland excess water drainage channels can be found. Detailed along- and cross section data was available from the Sóstó main channel in the database maintained by the Lower Tisza District Water Directorate (ATIVIZIG). All other channels were digitized based on RapidEye satellite imagery and cross sections were derived from the digital elevation model to create the geometrical model of the area.

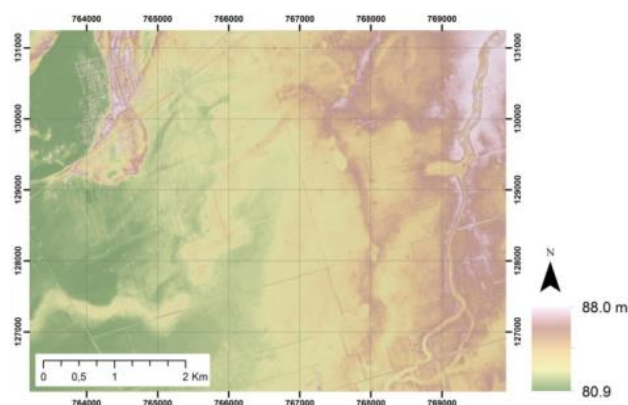


Figure 3. The LIDAR based digital elevation model covering the extent of the study area.

### 2.2.4. Precipitation

The key component of catchment models is the amount of rainfall in the area, since this is the main source of recharge. For this study, daily precipitation data from the measuring station in Székutas was supplied by the Lower Tisza District

Water Directorate.

### 2.2.5. Evaporation

The evaporation from vegetation as well as from the soil was taken into account (evapotranspiration). The determination of its exact quantity is a difficult task, especially for smaller catchments. Therefore, a constant value was used in the model, based on the long term average evapotranspiration data as published in Hungarian literature (Szász & Tőkei 1997).

### 2.2.6. Soil characteristics

The AGROTOPO database was used as source for the soil characteristics (Pásztor et al., 2013). This 1:100 000 scale database was originally created during the 1980s as a basis for regional-scale agro-environmental programs and analysis. For homogeneous agro-ecological units, it provides information on parameters like genetic soil type, soil parent material, soil texture, clay mineral composition, soil water content, acidity and carbon content, organic matter content, topsoil thickness, soil productivity value, inland excess water sensitivity, sensitivity to acidification, and sensitivity to compaction. The model incorporates the extent of the different soil types using polygons.

To model the unsaturated soil layers, data is needed about the depth of the different soils types, their water retention properties and their hydraulic conductivity. The most commonly used method for water retention properties are soil water retention (pF) curves, which give the relation between soil moisture suction and soil moisture content. For the three main soil types (sand, loam, clay) pF curves can be found in literature (Stefanovits et al., 2010)

### 2.2.7. Groundwater level

The groundwater level is the most important parameter of the saturated soil submodel. The groundwater level determines how much water can still infiltrate into the soil. When the groundwater level is higher than the bottom of the channel, the water will flow into the channel, while at lower groundwater levels, the water in the channels will infiltrate into the soil. This can be dynamically represented in the model; an initial groundwater level needs to be specified which is adapted continuously during the simulation. The initial condition can be specified as one absolute value for the total area or as a value relative to the height of the terrain. In the study area, a groundwater measuring station from the Lower Tisza District Water Directorate is located in Székutas. The initial conditions for the groundwater level were specified

based on its time series.

### 2.2.8. Calibration data

The data to calibrate the model were derived by processing a RapidEye satellite image of April 2013. RapidEye is a commercial satellite constellation consisting of five satellite platforms with uniform instruments. This allows for the continuous acquisition of visible to near infrared data in five different bands with a spatial resolution of 5 meter. The five satellites provide the opportunity for daily data collection from the same area. This is important in operational inland excess water monitoring since the phenomenon is very dynamic. Furthermore, since inland excess water is usually occurring in periods with lots of precipitation and clouds, it is often difficult to acquire a high quality image. The raw satellite image was atmospherically corrected to acquire surface reflectance data with minimal atmospheric disturbance.

The individual pixels of the image were converted into sets of pixels using a multi-resolution image segmentation approach. Several experiments were executed to reach the optimal settings for the segmentation procedure. Homogeneous sets of pixels were converted into vector objects, which were manually classified into different land cover classes (Fig. 4). Apart from an open water or inland excess water class, a saturated soil class was identified as well.

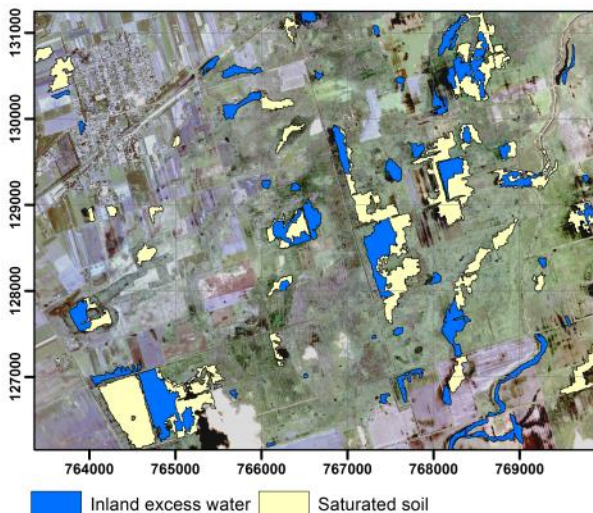


Figure 4. Calibration data derived from the RapidEye satellite image

## 3. MODELLING

During the first step, the model needs to be fed with the input data. Since the model handles the data independent from the spatial and temporal resolution, these are specified later.

### 3.1. Overland flow

To model the overland flow, the finite difference approach (Danish Hydraulic Institute 2014b) was selected from the available methods. Its parameters are:

- Surface roughness, which could be specified with a single value, because the land use in the area is homogeneous. The dynamics of the overland flow do not play a decisive role in inland excess water modelling, since the simulated velocity of the flow and the discharge are very small, and the model is relatively insensitive to this parameter. The specified values are between 5 and 10  $m^{1/3}/s$ .
- Detention storage, which is the minimal water depth before water will flow as sheet flow to the adjacent grid cell. The model was not sensitive to this parameter either for the same reason as for the surface roughness. The specified values are between 5 and 10 mm.

### 3.2. Evapotranspiration

The Kristensen-Jensen model (Danish Hydraulic Institute 2014b) was used to determine the evapotranspiration. The specified reference evapotranspiration was set to 1.86 mm/day (Gregory et al., 2003). The CORINE database was used to specify two different land use zones in the study area: natural grassland and non-irrigated arable land. One vegetation type was defined in the model, with a root depth of 1 000 mm and a leaf area index of 0.5.

#### 3.2.1. Unsaturated flow

Based on the AGROTOPO soil database, two soil types were added to the model. Water household and hydraulic parameters were specified based on scientific literature (Van Genuchten 1980, Van Genuchten et al., 1991).

The study showed the model is sensitive to these parameters, because they directly affect the near surface infiltration and transportation capabilities of the soil, and as such they directly influence the formation of inland excess water.

Figure 5 gives the results of the sensitivity analysis. The initial situation is shown in the figure at the top while a simulation ran on a soil with lower infiltration capacity is shown in the figure at the bottom. Changes result in a small increase in the size of the inundation, while the number of cells with saturated soil grew considerably. Therefore, it can be concluded that it is important to carefully specify these parameters, when setting up and calibrating the model.

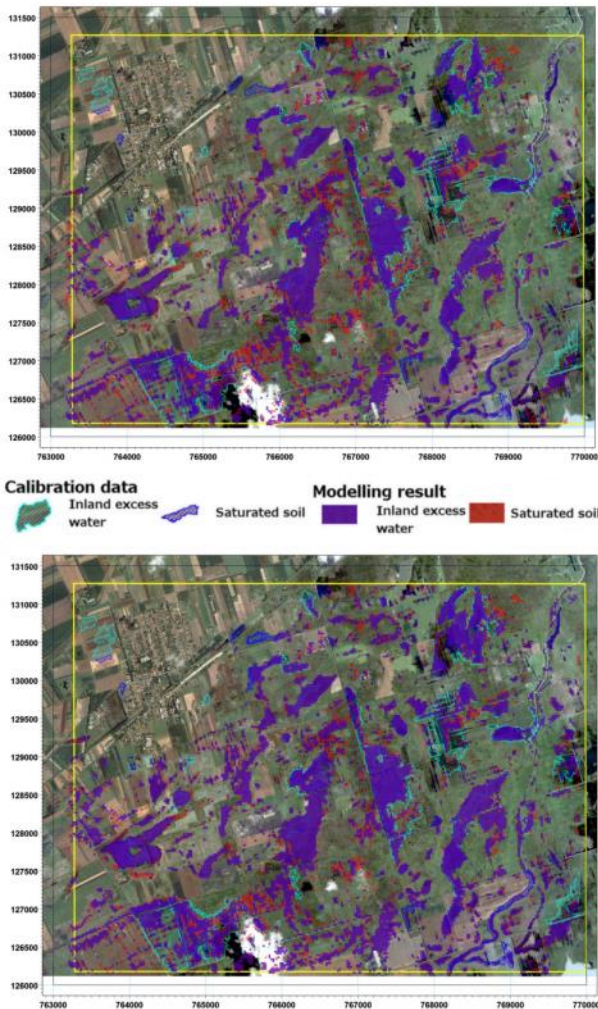


Figure 5. Sensitivity analysis on unsaturated soil (initial situation, top) and on unsaturated soil with lower infiltration capacity (bottom).

### 3.3. Saturated groundwater flow

The saturated soil layer is modelled as a separated soil layer with the following parameters:

- the horizontal and vertical hydraulic conductivity are both specified as  $1.7 \times 10^{-5}$  m/s
- the specific yield is 20%
- the specific storage is  $1.1 \times 10^{-4}$  m<sup>-1</sup>

The model shows similar sensitivity in case of two phased soil layers and three phased layers. Therefore these parameters should be added. They are not calibration parameters, but physical ones, which are the result of actual measurements.

### 3.4. Channel flow

Inland excess water drainage channels play a crucial role in the formation, location and size of the inundations in the study area. As mentioned before, only detailed data on the Sóstó main channel was

available for this research. In addition, also channels identified on the satellite images were digitized, but without an accurate survey the along- and cross sections can only be used conditionally.

The results of the modelling show that the influence of the drainage channels on the simulation is strong. Therefore, it is not possible to optimally calibrate the model without accurately measuring and mapping of the drainage network. Figure 6 shows a simulation result where the available capacity in the channels at the start of the precipitation period was specified as 20-30%, so the initial water level and the upper boundary conditions for the discharge were increased.

### 3.5. Spatial and temporal resolution

The model was executed with different settings for the spatial and temporal resolution, and for the length of the simulation period. The initial spatial resolution was 50 x 50 meter, which resulted

in a computational grid of 140 x 110 cells covering the study area of about 39 km<sup>2</sup>. This gives lower computational demands and faster simulations, but also a reduction of the spatial resolution of the elevation data, which means a considerable decrease in information content. A 25 x 25 meter spatial resolution provides sufficient detail with acceptable calculations times (approx. 35 minutes, Intel Core i7-2760QM, 8 GB RAM, MIKE SHE 2014 64 bit) for the selected 40 day calculation period and 24 hour time step.

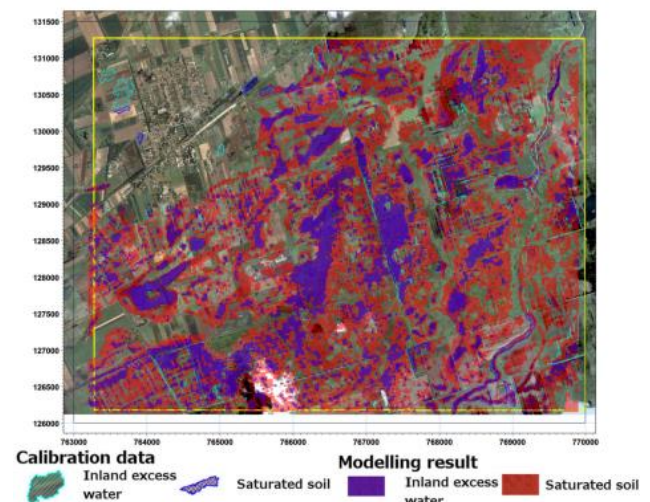


Figure 6. Simulation result with increased initial water levels.

A smaller spatial resolution results in reduced computations time steps due to stability problems, and then - not only because of the larger number of computational cells, but also because of the

compression of the time discretization - the calculation time increases.

The calculation period was defined from 1 March 2014 until 9 April 2014. This period covers the 40 days before the acquisition of the satellite image. The simulation results would have been erroneous for an earlier calculation period, because the long term average temperature for February in the study area is about  $-5\text{ }^{\circ}\text{C}$  and the snow module - although available in the software - was not used.

Figure 7 shows the results for an individual grid cell for two different simulation periods (One starting on January 26 and the other on February 28). For the first period, three different infiltration capacity settings have been tried while, for the second period four different settings were used. It can be seen that within about one month the groundwater level is at the same level for all simulations, indicating that there is no need to take a longer calculation period into account.

#### 4. VALIDATION

The modelling results were validated using an independent validation data set that was created by digitizing reference inland excess water inundations from the RapidEye satellite image of 8 April 2014 (Fig. 8).

The inundations were visually identified. It is practically impossible to distinguish between saturated soil and open water on the satellite image; therefore these two classes were combined. The reference inland excess water polygons were rasterized and crossed with the pixels with a positive value in the modelling result.



Figure 7. Results of two simulation periods, and different infiltration capacity settings.

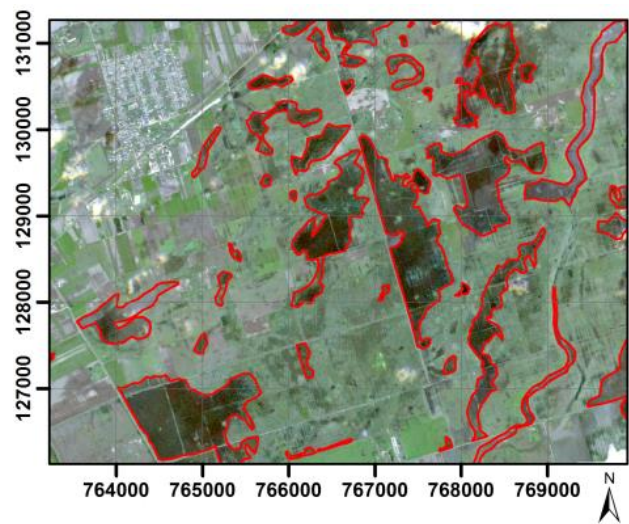


Figure 8. Reference inland excess water patches on the RapidEye satellite image.

Table 1 provides an overview of the validation results. The overall accuracy of all simulation is above 75% (Congalton 1991). The user accuracy – indicating the probability that an inland excess water patch in the result map indeed would have been inland excess water in the input data set – is relatively low for all dates due to a large amount of false positives. These are pixels classified as inland excess water but were in reality a different class. A reason for this might be that the combined inland excess water and saturated soil class in the reference data was taken to small, meaning that the area with saturated soil was not completely added to the reference data.

Especially in the centre of the image where dark colour is visible (Fig. 8), this may have happened. The producer accuracy – indicating the probability that an inland excess water patch in the input data set is properly classified as inland excess water in the result map – is the highest for 6<sup>th</sup> April, when the largest area of inland excess water was simulated.

Table 1. Simulation validation.

Simulation date:	Overall accuracy (%)	User accuracy (%)	Producer accuracy (%)
6 April	76	39	60
7 April	81	47	52
8 April	82	45	51
30 June	81	49	48

A quantitative evaluation of the simulation result is shown in figure 9, where the simulation results are overlaid with the validation data.

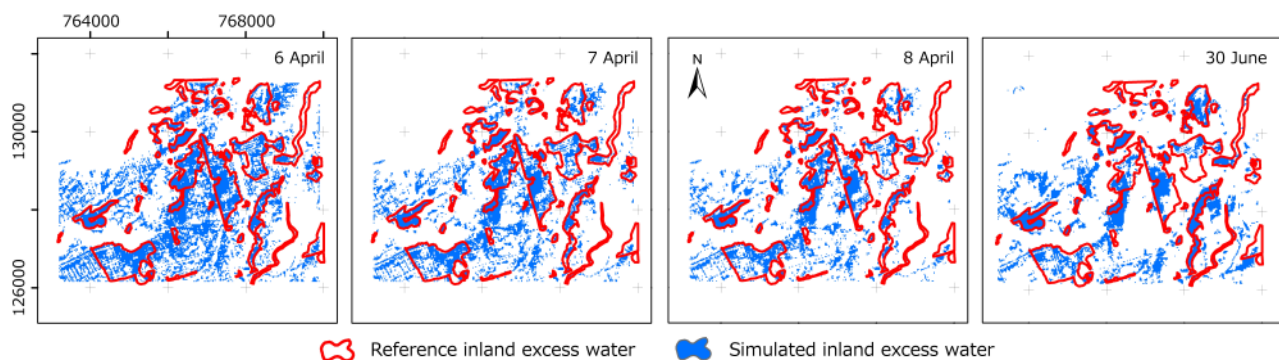


Figure 9. Simulation results on 4 different days overlaid with the reference data.

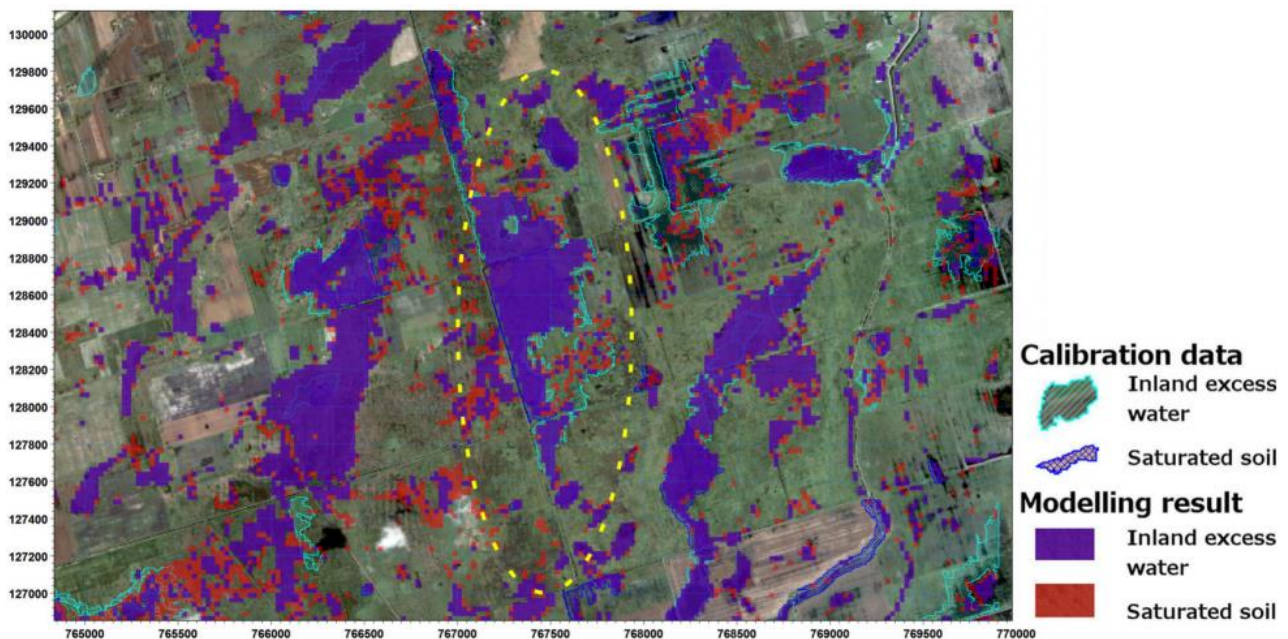


Figure 10. Results of the final calibration.

The validation data consists of polygons with inland excess water as well as saturated soil polygons. The simulation results consist of continuous values indicating the range between saturated soil and inundation. It can be seen that the total amount of modelled inland excess water decreases in time. This reduces the amount of false positives, but also decreases the producer accuracy.

In figure 10, the cyan (saturated soil) and dark blue (inundation) shaded polygons are the result of the satellite processing, while the red (saturated soil) and purple (inundation) pixels are the modelled results.

In the area in the centre (indicated with the yellow, dashed line), the calculated results correspond well with the calibration data. Here, detailed data was available about the inland excess water drainage channel. Other areas, with less accurate channel data show large errors in the modelling results.

## 5. CONCLUSIONS

The results of the simulations show that modelling inland excess water inundations based on physical parameters provide reasonable results and that satellite imagery can be used for its calibration. The over-estimation of inland excess water may be due to conservative sampling of the saturated soil class in the reference data. The simulated inundations at later dates better coincide with the reference data. The results also show that the determination of hydraulic and water balance parameters of the soil, as well as accurate data on the complete drainage network in the study area are of decisive importance. Without these, it is not possible to calibrate the model.

Hydrological modelling inland excess water floods based on physical data gives satisfying results although these are highly dependent on the available input data. Compared to the commonly used GIS modelling approaches and remote sensing techniques, this method does not require determination of weighing factors, nor does it rely on the availability of digital imagery. It only depends on the specification of the physical input parameters. It also provides a method to predict the extent, location and duration of inland excess water, which is not possible with other methods. The model can be applied to areas with similar conditions as well.

The sensitivity analyses show that – apart from the ridges in the terrain – the model is sensitive to soil and vegetation characteristics. The exact determination of the influence of these parameters requires more research.

### Acknowledgements

The help and data provided by the colleagues of the Lower Tisza District Water Directorate (ATIVIZIG) are highly appreciated.

### REFERENCES

- Barta, K. - Szatmári, J. - Posta, Á.,** 2011. *Connection between inland water development and motorways*. XIV. Congress of Hungarian Geomathematics and the Third Congress of Croatian and Hungarian Geomathematics, Mórahalom, 1–8
- Bozán Cs, Körösparti J. & Pásztor, L.,** 2009. *GIS-based Mapping of excess water inundation hazard in Csongrád county (Hungary)*, Proceedings of the International Symposia on Risk Factors for Environment and Food Safety & Natural Resources and Sustainable Development, Oradea, 678–684.
- Congalton R.G.,** 1991. *A review of assessing the accuracy of classifications of remotely sensed data*, Remote Sensing of Environment, 37, 1, 35–46
- Csornai G., Lelkes M., Nádor G. & Wirnhardt Cs.,** 2000. *Operatív árvíz- és belvív- monitoring távérzékeléssel*. (Operative flood and inland excess water monitoring using remote sensing) (in Hungarian). Geodézia és Kartográfia 52/5, 6-12
- Danish Hydraulic Institute (DHI),** 2014a. *MIKE SHE User Manual, Volume 1: User Guide*, 370 p.
- Danish Hydraulic Institute (DHI),** 2014b. *MIKE SHE User Manual, Volume 2: Reference Guide*, 444 p.
- Davie T.,** 2008. *Fundamentals of Hydrology*. New York: Routhledge, 200 p.
- Gál N. & Farsang A.,** 2013. *Weather extremities and soil processes: impact of excess water on soil structure in the South Hungarian Great Plain*. In: Lóczy D. ed. *Geomorphological Impacts of Extreme Weather: Case Studies from Central and Eastern Europe*. Springer, Heidelberg, 313-325
- Kristensen K. J. & Jensen, S. E.,** 1975. *A model for estimating actual evapotranspiration from potential evapotranspiration*, Nordic Hydrology 6, 3, 170–188
- Kling Z. & Bálint G.,** 2009. *Mapping excess water inundation induced hazard and its importance in Hungary*, Riscuri si Catastrofe, 8, 7, 159–166.
- Kuti L, Kerék B. & Vatai J.,** 2006. *Problem and prognosis of excess water inundation based on agrogeological factors*, Carpathian Journal of Earth and Environmental Sciences 1, 1, 5 – 18.
- Mezősi G, Bata T, Meyer B, Blanka V. & Ladanyi Zs,** 2014. *Climate Change Impacts on Environmental Hazards on the Great Hungarian Plain, Carpathian Basin*. International journal of disaster risk science, 5, 2, 136-146.
- Mucsi, L. & Henits, L.,** 2010. *Creating excess water inundation maps by sub-pixel classification of medium resolution satellite images*. Journal of Environmental Geography, 3, 1–4, 31–40.
- Graham D.N. & Butts M.B.,** 2005. *Flexible integrated watershed modeling with MIKE SHE*. *Watershed Models*. In: V.P. Singh and D.K. Frevert, eds. Water Resources Publication, Highlands Ranch, CO 245–272.
- Gregory P. A., Scurlock J.M.O. & Hicke J.A.,** 2003. *Global synthesis of leaf area index observations: implications for ecological and remote sensing studies*. Global Ecology & Biogeography, 12, 191–205.
- Pásztor, L., Szabó J., Bakacsi Zs. & Laborczia A.,** 2013. *Elaboration and applications of spatial soil information systems and digital soil mapping at Research Institute for Soil Science and Agricultural Chemistry of the Hungarian Academy of Sciences*. Geocarto International, 28, 1, 13-27.
- Pásztor, L., Körösparti J., Bozán Cs., Laborczia A. & Takács K.,** 2014. *Spatial risk assessment of hydrological extremities: Inland excess water*

- hazard, Szabolcs-Szatmár-Bereg County, Hungary. Journal of Maps.
- Priest, S. J., Parker D. J., Hurford A. P., Walker J. & Evans K.**, 2011. *Assessing options for the development of surface water flood warning in England and Wales*. Journal of Environmental Management, 92, 12, 3038–3048.
- Rakonczai J, Farsang A., Mezősi G. & Gál N.**, 2011. A belvízképződés elméleti háttere (Theoretical background of inland excess water formation) (in Hungarian), Földrajzi Közlemények 135, 4, 339-350.
- Romanescu G.**, 2009. *Siret river basin planning (Romania) and the role of wetlands in diminishing the floods*. WIT Transaction on Ecology and the Environment, 125, 439-453.
- Romanescu G., Stoleriu C. & Zaharia C.**, 2011. *Territorial Repartition and Ecological Importance of Wetlands in Moldova (Romania)*. Journal of Environmental Science and Engineering, 5, 11, 1435-1444.
- Stefanovits P., Filep Gy. & Füleky Gy.**, 2010. *Talajtan.*(Soil science) (in Hungarian) Budapest: Mezőgazda kiadó. 470 p.
- Szatmári J., Szíjj N., Mucsi L., Tobak Z., Van Leeuwen B., Lévai Cs., & Dolleschall J.**, 2012. *Comparing LIDAR DTM with DEM-5 of Hungary*. In: J. Geiger, E. Pál Molnár, T. Malvic, eds. New horizons in Central European geomathematics, geostatistics and geoinformatics. Szeged: Institute of Geosciences, University of Szeged, 151–158.
- Szatmári J. & Van Leeuwen B. (eds)**, 2013. *Inland Excess Water – Belvíz – Suvišnje Unutrašnje Vode*, Szeged: Szegedi Tudományegyetem, Novi Sad: Újvidéki Egyetem, 154 p.
- Szász G. & Tőkei L. (eds)**, 1997. *Meteorológia mezőgazdáknek, kertészeknek, erdészeknek*. (Meteorology for farmers, gardeners, foresters) (in Hungarian), Budapest: Mezőgazda Kiado, 722 p.
- Túri Z. & Szabó G.**, 2012. *A nyírség felszíni hidrológiai viszonyainak térképezése kvantitatív adatbázisok és űrfelvételek alapján*. (Mapping of the hydrological situation of the Nyírség based on quantitative databases and satellite imagery) (in Hungarian) In: D. Nyári, ed. Kockázat - Konfliktus – Kihívás. Szeged: SZTE TTK Természeti Földrajzi és Geoinformatikai Tanszék, 921-930.
- Van Genuchten, M.Th.**, 1980. *A closed-form equation for predicting the hydraulic conductivity of unsaturated soils*. Soil Sci. Soc. Am. J., 44, 892–898.
- Van Genuchten, M.Th., Leij, F.J. & Yates, S.R.**, 1991. *The RETC code for quantifying the hydraulic functions of unsaturated soils*. U.S. Salinity Laboratory, USDA, ARS, Riverside, California
- Van Leeuwen, B.**, 2012. *Artificial neural networks and geographic information systems for inland excess water classification*. PhD dissertation, University of Szeged, Szeged, 111 p.
- Van Leeuwen, B, Mezősi G., Tobak Z., Szatmári J. & Barta K.**, 2012. *Identification of inland excess water floodings using an artificial neural network*, Carpathian Journal of Earth and Environmental Sciences 7, 4, 173-180.

Received at: 16. 09. 2015

Revised at: 04. 04. 2016

Accepted for publication at: 26. 04.2016

Published online at: 12. 05. 2016